CONEM2014
VIII CONGRESSO NACIONAL DE ENGENHARIA MECÂNICA
UBERLÂNDIA - MG - BRASIL 10 A 15 DE AGOSTO DE 2014

CONTINUOUS OPTIMIZATION OF DISCRETE MODAL FILTERS APPLIED TO FLEXIBLE STRUCTURES

Augusto Hirao Shigueoka, augusto.shigueoka@usp.br[1]
Marcelo Areias Trindade, trindade@sc.usp.br[1]

[1]Universidade de São Paulo, Av. Trabalhador Sancarlense, 400, 13566-590, São Carlos, SP, Brasil

Abstract: *Modal control stands out as a very convenient technique in vibration suppression, since it lets the control engineer individually pick up the modes of interest. This can potentially also reduce required control effort and spillover instabilities. Since the seminal work of Meirovitch in the early 80s, several authors have proposed different ways of implementing modal and semi-modal control techniques. The main issues to be solved are, on the one hand, how to isolate the response of a given vibration mode and, on the other hand, how to actuate only on a given vibration mode. For the sensor problem, it should be possible to isolate one vibration mode of a flexible structure by using just one sensor as long as both carefully designed observer and filters are used. However, it may be also possible to simply use a modal sensor that will filter out the undesirable modes, while detecting those of interest. Despite being relatively well explored, the previous works found in the open literature on modal sensors always considered a finite number of frequencies sampled from the discrete sensors' Frequency Response Function (FRF). Therefore, the optimal results may depend on the frequency range discretization. In this work, an extension to the previous method uses a continuous formulation for both displacement field and sensors' FRFs in order to model the flexible structure of interest and the modal sensor behaviors. From the derived equations, an objective function that reflects the difference between the modal sensor output and its ideal signal is formulated. As a result, it is possible to make use of non-linear optimization programming in order to seek the optimal modal sensor configuration.*
Keywords: *modal filter, optimization, distributed parameter, observation spillover*

1. INTRODUCTION

Some fields of study, such as aerospace and automobile engineering, strive to reduce the weight of their structures while keeping safety and comfortability under tolerable margins. Therefore, those structures tend to be much more flexible than the usual ones used in everyday designs. Due to these weight constraints, the use of vibration control techniques, albeit expensive, becomes feasible. In fact, a lot of research has been done in this area from the 1970's until the 1990's, stimulated by the Space Race. The Cold War has already long ended, but the techniques developed in the field of vibrations are still used in the industry.

The Independent Modal Space Control (IMSC) is a particularly interesting method to suppress the oscillations of a flexible structure developed by Meirovitch and Baruh (1982). Differently from the simpler negative velocity feedback, it is possible to reallocate the poles of each mode of vibration individually. This way, it is ideally possible to change the dynamical behavior of the structure irrespective of how demanding the requirements of the project may be. Unfortunatelly, the detection and control of all modes of interest must obey predefined conditions, such as observability and controlability, as stated by Balas (1978). Even though those conditions allow the project of a control system comprising one sensor and one actuator only, it will be necessary to design not only an observer that reconstructs the state of the system from just one sensor but also a control law that reasonably affects all modes of interest. As a result, the designer will have to use either an observer based on a sufficiently accurate model of the structure or a stochastic estimator, such as the Kalman filter. Besides, Balas also investigated the effects of observation and control spillover on the stability of the residual modes. It turned out that while the presence of both observation and control spillover may lead to instability, it is possible to tolerate control spillover alone. The performance of the control system will degrade, but at least it is possible to avoid unstable closed loop systems.

The use of comb filters is one of the alternatives that can be used in order to remove observer spillover. Modal sensors stand out as another approach. Instead of designing a comb filter and a potentially complex observer, modal sensors atenuate residual modes by just using linear combinations of the signals provided by several discrete sensors distributed over the structure, as ilustrated in Fig. 1 the readings of the various sensors are then multiplied by individual gains and summed. Then by changing the values of these gains it is possible to manipulate the final signal so as to approximate the ideal signal. Despite increasing the cost of the equipment, due to the higher number of sensors and actuators, the observer in the control law is exchanged for a hardware that may be constructed from simple electronic components, avoiding

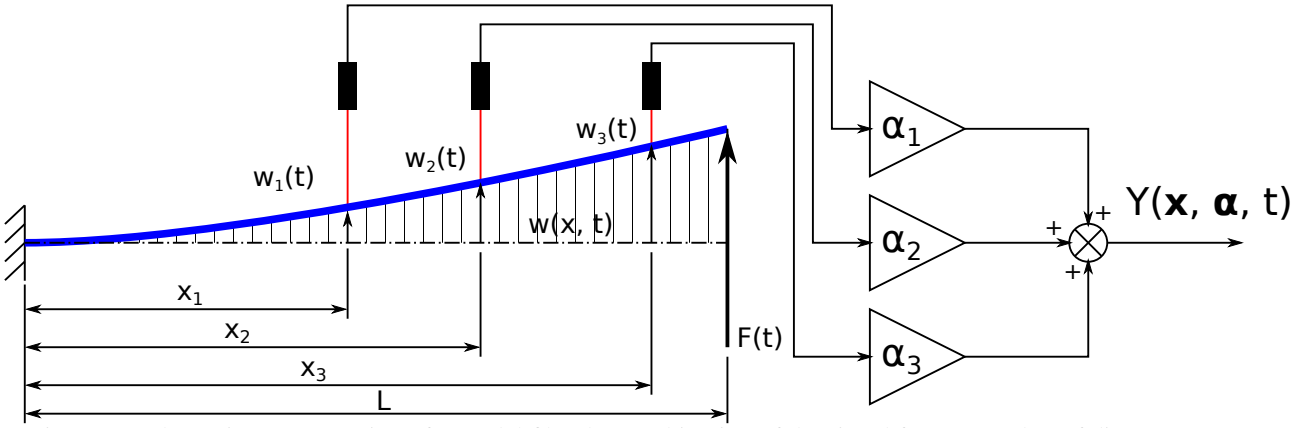

Figure 1: Schematic representation of a modal filter by combination of the signal from a number of discrete sensors.

the use of microprocessors. The design of discrete modal sensors depend basically of two parameters: the position and the gain of each discrete sensor. Some techniques have been developed in order to find the best design, such as the pseudo-inverse used by Preumont *et al.* (2003), which consists basically of finding the Least Squares solution, and genetic algorithm fomulations, such as the ones by Han and Pagani Jr. (Han and Lee, 1999;Pagani Jr and Trindade, 2009). As a motivation for further investigation in this subject, Fig. 2 compares magnitude of the FRF of the modal sensor designed from the LSQ method and the FRF of a single sensor placed at the tip of the beam. The red line corresponds to the response of a sensor at the free tip of a cantilever beam, while the green one to the response of the modal sensor optimized by the method described in this work to detect the first four modes and supress the other ones. Both of the responses should match the ideal sensor signal depicted in dashed black line. As may be noticed from the resonance peaks, the modal sensor is more uniform in the modes that should be detected, with gains almost equal to 0dB (100%) in the desired modes and residues under -20dB (10%) in the remaining of the frequencies. The sensor at the tip does not allow such control. Moreover, the region at the left of the figure shows another interesting characteristic of modal sensors: they can keep minimal phase for the desired modes.

As noted by Friswell (2001), the performance of the modal sensor depends heavily on the number and positioning of individual sensors. While it is possible to create a grid of sensors over a structure and change each gain as necessary, as Preumont *et al.* (2003) did, Pagani Jr and Trindade (2009) have shown that one could also try to use a reduced number of sensors without greatly affecting the overall preformance if an optimal placement granted that possibility. Still, most of the searched methods employed a formulation for the objective function that was based on a finite element model and a finite number of samples from each sensor's FRF. The objective function in this work is based on a continuous formulation for both the displacement fields and the FRFs. As a result, the objective function may be minimized by non-linear programming optimization methods with availability of the exact formulation of its gradient vector. As of the writing of this paper, however, an analytical expression for the integrals in the formulation had not been calculated and all of them were numerically computed.

This work investigated the optimization of a modal sensor on a uniform cantilever beam. The dynamic model was constructed from the Ritz-Galerkin method using expansion by eigenfunctions, resulting in an analytical description of the system. Then, the objective function could be defined in terms of the difference between the modal sensor signal and the target signal. The modal sensor in this study took four different readings along the beam and tried to identify the first four modes of vibration. In order to account for spatial aliasing, the first 12 modes of vibration were included in the dynamic model.

After finishing the formulation of both the objective function and its gradient, the problem was optimized through

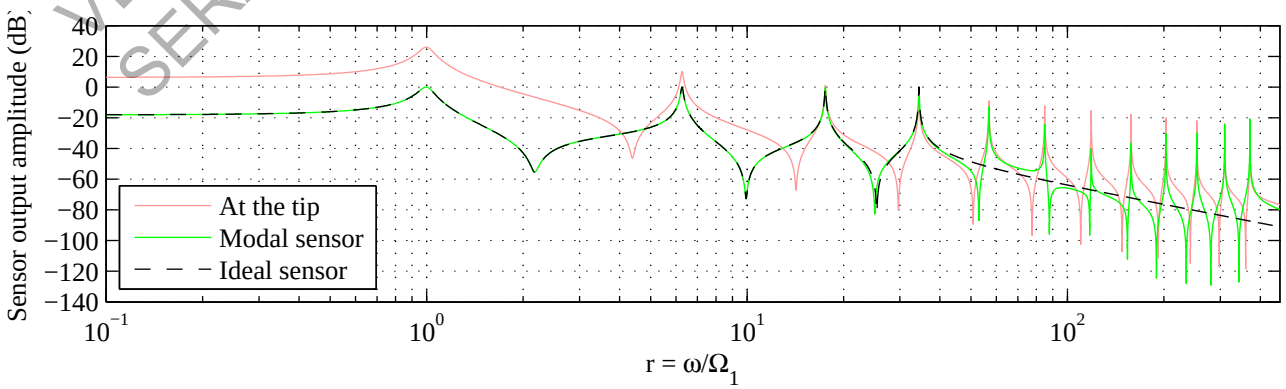

Figure 2: FRF of output signal obtained from a displacement sensor at the beam tip and from a modal filter with four discrete displacement sensors compared to an ideal filtered output that isolates the first four resonances.

the function `fmincon` available in the MATLAB Optimization Toolbox. The interior point method was chosen, with the Hessian matrix estimated by the Broyden-Fletcher-Goldfarb-Shanno (BFGS) algorithm. More details on the optimization method may be found in Rao (2009).

Non linear optimization problems are generally subject to multiple local minima. This case was not an exception. The method stopped at several different stationary points. As a countermeasure, a second optimization procedure considering several different starting points was carried on and the configuration corresponding to the lowest value of the objective function was chosen.

2. MODELING OF A CANTILEVER BEAM WITH SEVERAL DISCRETE DISPLACEMENT SENSORS

The studied system consisted of a cantilever beam using the Euler-Bernoulli formulation. The beam is made from an isotropic material whose modulus of elasticity E, Poisson's ratio ν and density ρ are uniformly distributed. The cross-section is constant, with area A and second moment of area I. The left extremity is clamped while the right one is free, excited by an harmonic point force $F_L(t)$. The distributed load $f(x,t)$ and the point moment M_L are null in this study. Such model is one of the simplest that will still show infinite modes of vibration and was chosen as a benchmark for this optimization process. The well known Euler-Bernoulli formulation can easily be found in the literature. This worked was based on the formulations described in (Meirovitch, 1990; Meirovitch, 1996; Géradin and Rixen (1997)).

2.1 Governing equations

The Partial Differential Equation (PDE) as well as the Boundary Conditions (BCs) obtained from the application of Hamilton's principle to the cantilever beam are as follow:

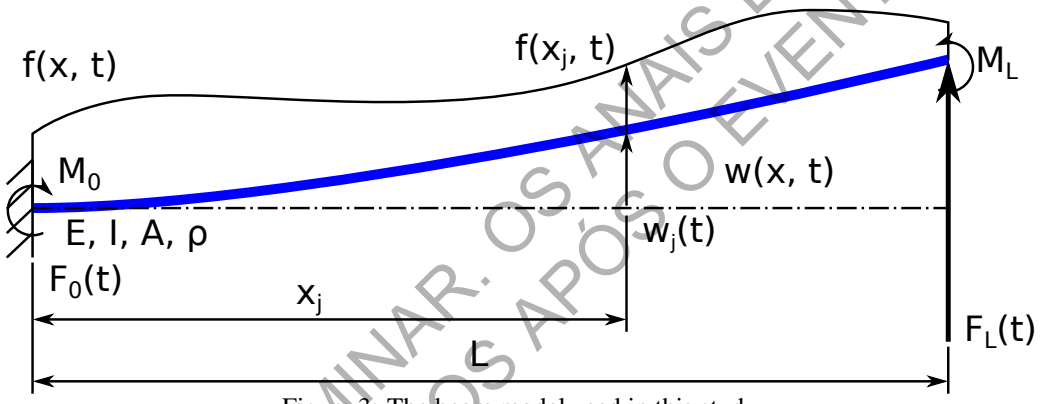

Figure 3: The beam model used in this study

PDE:

$$\frac{\partial^2 \eta}{\partial \tau^2} + \frac{1}{\beta_1^4}\frac{\partial^4 \eta}{\partial \xi^4} = \gamma(t) \tag{1}$$

BCs:

$$\left.\frac{\partial \eta}{\partial \xi}\right|_{\xi=0} = 0 \tag{2a}$$

$$\left.\left(\frac{\partial^2 \eta}{\partial \xi^2} - \frac{LM_L}{EI}\right)\right|_{\xi=1} = 0 \tag{2b}$$

$$\left.\eta\right|_{\xi=0} = 0 \tag{2c}$$

$$\left.\left(\frac{\partial^3 \eta}{\partial \xi^3} + \frac{L^2 F_L}{EI}\right)\right|_{\xi=1} = 0 \tag{2d}$$

Where:

$$\xi = \frac{x}{L} \quad \tau = \Omega_1 t \quad \eta(\xi,\tau) = \frac{w(x,t)}{L} \quad \gamma = \frac{f(\xi,\tau)}{\beta_1^4} \quad \Omega_1 = \frac{1}{L^2}\sqrt{\beta_1 \frac{EI}{\rho A}}$$

are the adimensionalised variables of the system. Most of the variables were shown in Fig. 3. β_1 and Ω_1 are constants used in the adimensionalisation ot the variables. They are, respectively, the eigenvalue and the natural frequency associated to the beam's first mode of vibration. This Initial Boundary Value Problem (IBVP) can be solved by eigenfunction expansion, requiring the solution of the associated Sturm-Liouville problem solvable by separation of variables $\eta(\xi,\tau) = \Phi(\xi)C(\tau)$, yielding the normalised eingenfunctions:

$$\Phi_j(\xi) = k_j\left[s_2(\beta_j\xi) - \frac{s_1(\beta_j)}{c_1(\beta_j)}c_2(\beta_j\xi)\right], \quad j = 1,2,3,\ldots \tag{3}$$

Where:

$$s_1(\xi) = sin(\xi) + sinh(\xi)$$
$$c_1(\xi) = cos(\xi) + cosh(\xi)$$
$$s_2(\xi) = -sin(\xi) + sinh(\xi)$$
$$c_2(\xi) = -cos(\xi) + cosh(\xi)$$
$$k_j = \left\{ \int_0^1 \left[s_2(\beta_j \xi) - \frac{s_1(\beta_j)}{c_1(\beta_j)} c_2(\beta_j \xi) \right]^2 d\xi \right\}^{-\frac{1}{2}}$$

And each of the β_j is a solution of the equation:

$$c_1(\beta_j)^2 - s_1(\beta_j) s_2(\beta_j) = 0$$

The $\Phi_j(\xi)$ as defined in Eq. (3) will be used as the orthogonal base in the Ritz-Galerkin method that will reduce the order of the system, so that its dynamical response can be computed.

2.2 Order Reduction by Ritz-Galerkin

The approximated displacement field, denoted by $\hat{\eta}(\xi, \tau)$, consists of a linear combination of a finite number of normalized shape functions: $\Phi_j(\xi)$.

$$\eta(\xi, \tau) \approx \hat{\eta}(\xi, \tau) = \sum_{j=1}^{m} \Phi(\xi) q(\tau)$$

In this study, the 12 modes of vibration were included in the dynamic model of the beam, so $m = 12$. The previous equation also has a more compact notation:

$$\hat{\eta}(\xi, \tau) = \mathbf{\Phi}(\xi)^T \mathbf{q}(\tau) \tag{4}$$

Where:

$$\mathbf{\Phi}(\xi) = \begin{bmatrix} \Phi_1(\xi) \\ \Phi_2(\xi) \\ \vdots \\ \Phi_m(\xi) \end{bmatrix} \quad \mathbf{q}(\tau) = \begin{bmatrix} q_1(\tau) \\ q_2(\tau) \\ \vdots \\ q_m(\tau) \end{bmatrix}$$

The substitution of $\eta(\xi, \tau)$ by $\hat{\eta}(\xi, \tau)$ in Eq. (1) with the help of Eq. (4) followed by the Ritz-Galerkin method yields a system of uncoupled Ordinary Differential Equations (ODEs):

$$\mathbf{I} \frac{\partial^2 \mathbf{q}}{\partial \tau^2} + \mathbf{\Lambda} \frac{\partial \mathbf{q}}{\partial \tau} + \mathbf{\Omega}^2 \mathbf{q} = \mathbf{F} \tag{5}$$

Where:

$$\mathbf{I} = \int_0^1 \mathbf{\Phi} \mathbf{\Phi}^T d\xi$$
$$\mathbf{\Omega}^2 = \frac{1}{\beta_1^4} \int_0^1 \frac{\partial^2 \mathbf{\Phi}}{\partial \xi^2} \frac{\partial^2 \mathbf{\Phi}}{\partial \xi^2}^T d\xi$$
$$\mathbf{F} = \int_0^1 \mathbf{\Phi} \gamma d\xi + \mathbf{\Phi}|_{\xi=1} \frac{L^2 F_L}{EI}$$

2.3 Modal Sensor Signal

From the calculated matrices it is possible to formulate the system response to an external harmonic excitation $F(\tau)$ that consists of its magnitude $\tilde{\mathbf{F}}$ and variation over time $e^{ir\tau}$.

$$\mathbf{F}(\tau) = \tilde{\mathbf{F}} e^{ir\tau} \tag{6}$$

The complete solution includes both the transient and the steady-state parcel. In the frequency domain analysis, only the steady-state solution is considered. The coefficients of the eigenfunctions in the steady-state solution will represented as:

$$\mathbf{q}(\tau) = \tilde{\mathbf{q}}(r) e^{ir\tau} \tag{7}$$

Where $\tilde{\mathbf{q}}$ represents both magnitude and phase of the steady-state solution $\mathbf{q}(\tau)$. After substituting $\mathbf{q}(\tau)$ and $\mathbf{F}(\tau)$ in Eq. (5) for the expressions in Eqs. (6) and (7), the components for the frequency response are then found:

$$\left(-r^2\mathbf{I} + ir\mathbf{\Lambda} + \mathbf{\Omega}^2\right)\tilde{\mathbf{q}}e^{ir\tau} = \tilde{\mathbf{F}}e^{ir\tau}$$
$$\tilde{\mathbf{q}}(r) = \left(-r^2\mathbf{I} + ir\mathbf{\Lambda} + \mathbf{\Omega}^2\right)^{-1}\tilde{\mathbf{F}} \tag{8}$$

Recalling that the approximate displacement field $\eta(\xi,\tau)$ has got $\mathbf{q}(\tau)$ in its formulation, this variable can be substituted for its expression in Eq. (7).

$$\hat{\eta}(\xi,\tau) = \mathbf{\Phi}(\xi)^T\mathbf{q}(\tau)$$
$$\hat{\eta}(\xi,\tau) = \mathbf{\Phi}(\xi)^T\tilde{\mathbf{q}}(r)e^{ir\tau}$$
$$\hat{\eta}(\xi,\tau) = \tilde{\eta}(\xi,r)e^{ir\tau}$$
Where:
$$\tilde{\eta}(\xi,r) = \mathbf{\Phi}(\xi)^T\tilde{\mathbf{q}}(r)$$

By substituting $\tilde{\mathbf{q}}(r)$ in this last equation for the expression in Eq. (8), then $\tilde{\eta}(\xi,r)$, the FRF of the beam at a point ξ, is found.

$$\tilde{\eta}(\xi,r) = \mathbf{\Phi}(\xi)^T\left(-r^2\mathbf{I} + ir\mathbf{\Lambda} + \mathbf{\Omega}^2\right)^{-1}\tilde{\mathbf{F}} \tag{9}$$

Then the signal of the modal sensor, which is the linear combination of the FRF from several sensors distributed along the structure, can be defined as:

$$Y(\mathbf{\Xi},\mathbf{a},r) = \sum_{j=1}^{p}\alpha_j\tilde{\eta}(\xi_j,r) = \mathbf{a}^T\begin{bmatrix}\tilde{\eta}(\xi_1,r)\\ \tilde{\eta}(\xi_2,r)\\ \vdots\\ \tilde{\eta}(\xi_p,r)\end{bmatrix} \tag{10}$$

Where p is the number of sensors, $\mathbf{\Xi} = [\xi_1,\ldots,\xi_p]^T$ and $\mathbf{a} = [\alpha_1,\ldots,\alpha_p]^T$. In this study, four sensors were considered, which means $p = 4$. After substituting $\tilde{\eta}(\xi,\tau)$ for the in Eq. (9), the formula of the modal sensor FRF is finally found:

$$Y(\mathbf{\Xi},\mathbf{a},r) = \mathbf{a}^T\begin{bmatrix}\mathbf{\Phi}^T(\xi_1)\\ \mathbf{\Phi}^T(\xi_2)\\ \vdots\\ \mathbf{\Phi}^T(\xi_p)\end{bmatrix}\left(-r^2\mathbf{I} + ir\mathbf{\Lambda} + \mathbf{\Omega}^2\right)^{-1}\tilde{\mathbf{F}}$$

Another representation, with sum operators, would be:

$$Y(\mathbf{\Xi},\mathbf{a},r) = \sum_{j=1}^{p}\alpha_j\sum_{k=1}^{m}\Phi_k(\xi_j)P_k(r) \tag{11}$$

Where: $P_k(r) = \dfrac{1}{\Omega_k^2 - r^2 + ir\lambda_k}$ (12)

3. OBJECTIVE FUNCTION

3.1 Formulation

In order to define an objective function, it was necessary to define a reference signal that would represent the ideal performance of the modal sensor. This function is represented as a sum of several FRFs obtained from mass-spring-damper, following the formulation used by Preumont *et al.* (2003).

$$G(r) = \sum_{j=1}^{n}\frac{\lambda_j r_j}{r_j^2 - r^2 + i\lambda_j r} \tag{13}$$

Where n is the number of ressonances to be identified. The goal in this work is to identify the first 4 ressonances, so $n = 4$ and each parcel in Eq. (13) was calculated in order to approximate the first 4 ressonances in the model as much as possible.

Its desirable to make the modal sensor signal $Y(\mathbf{\Xi},\mathbf{a},r)$ as similar as possible to $G(r)$. For this reason, the metric that determines how close those two functions are has been defined as the error $E(\mathbf{\Xi},\mathbf{a},r)$ between the obtained signal and the ideal one:

$$E(\mathbf{\Xi},\mathbf{a},r) = Y(\mathbf{\Xi},\mathbf{a},r) - G(r)$$

The integral of the error function $E(\boldsymbol{\Xi}, \mathbf{a}, r)$ over the frequency range does not always return a reliable measure of the difference between the curves, though. A non null error may result in a null integral depending on its value over the domain. Consequently, the integral of the squared norm of the error will be used as the objective function:

$$f_c(\boldsymbol{\Xi}, \mathbf{a}) = \int_{r_{min}}^{r_{max}} E(\boldsymbol{\Xi}, \mathbf{a}, r)\bar{E}(\boldsymbol{\Xi}, \mathbf{a}, r)dr$$

From this point on integrals such as the one above will appear all the time. As a more compact notation, the internal product between two complex functions in this work is defined as:

$$\langle f, g\rangle = \int_{r_{min}}^{r_{max}} f(r)\bar{g}(r)dr \tag{14}$$

As a result, the objective function has a more compact notation:

$$f_c(\boldsymbol{\Xi}, \mathbf{a}) = \langle E(\boldsymbol{\Xi}, \mathbf{a}), E(\boldsymbol{\Xi}, \mathbf{a})\rangle$$

Despite the simpler appearance of the previous equation, it is easier to calculate the gradient ∇f_c from the expanded version:

$$f_c = \int_{r_{min}}^{r_{max}} \left[\sum_{j=1}^{p}\alpha_j \sum_{k=1}^{m}\Phi_k(\xi_j)\tilde{F}_k P_k(r) - G(r)\right] \cdot \left[\sum_{j=1}^{p}\alpha_j \sum_{k=1}^{m}\Phi_k(\xi_j)\tilde{F}_k \bar{P}_k(r) - \bar{G}(r)\right] dr \tag{15}$$

Note that at this point one important simplification has been made. Only real α_j were used, that is $\alpha_j \in \mathbb{R}, \quad j = 1, 2, \ldots, p$. Despite imaginary terms in α_j being theoretically possible, the gradient of the objective function ceases to have exclusively real components. Morevoer, the hardware implementation of a modal sensor with imaginary terms is not trivial. After admiting only real α_j, the gradient of f_c can be easily calculated:

$$\nabla f_c = \begin{bmatrix} \alpha_1 \left\langle \frac{\partial Y_1}{\partial \xi_1}, Y - G \right\rangle \\ \alpha_2 \left\langle \frac{\partial Y_2}{\partial \xi_2}, Y - G \right\rangle \\ \vdots \\ \alpha_p \left\langle \frac{\partial Y_p}{\partial \xi_p}, Y - G \right\rangle \\ \langle Y_1, Y - G\rangle \\ \langle Y_2, Y - G\rangle \\ \vdots \\ \langle Y_p, Y - G\rangle \end{bmatrix} \tag{16}$$

Where:

$$\frac{\partial Y_j}{\partial \xi_j} = \alpha_j \sum_{t=1}^{m} \left.\frac{\partial \Phi_k}{\partial \xi}\right|_{\xi=\xi_j} \tilde{F}_k P_k(r)$$

The Hessian of f_c has not been calculated analytically. Although it is possible to calculate its expression, such a task is quite laborous. Our optimization procedure configured `fmincon` so that it would estimate the Hessian from the BFGS method.

3.2 Sensibility to the target FRF parameters

One weak point in this objective function resides in the necessity of having at hands a set of accurately identified parameters of the system. In case it does not happen, the optimization will not be able to fit the sensor signal to the target FRF very well. Test cases were executed in order to show that effect qualitatively. All of then used the positioning obtained in the second optimization in 5.2 with the α_j recalculated so that the new target FRF would be accounted for.

In case the parameters of the target FRF are closely matched, the fitting will be almost perfect, as in Fig. 4b, where the gray curve represents the target FRF and the black curve the sensor FRF. In Fig. 4a, the modal damping factors of the target function $G(r)$ are equal to 0.5, which is half the value of this beam's damping factors, while in Fig. 4c the modal damping factor equals 0.2, that is, the double of the beam's damping factors. Although there is not much difference between the target function $G(r)$ and the modal filter output $Y(r)$, from the zoomed error plots in Fig. 5a and Fig. 5c it is evident how detrimental badly identified parameters are to the objective function. In both graphics the error may reach up to about -9.5dB (33%) while the correctly identified target function permits us to keep the error below -40dB (1%) for the first modes, as shown in Fig. 5b.

The objective funcion is similar to the identification method for lightly damped structures developed by Ewins and Gleeson (1982). Actually, the results in Fig. 4a are similar to the ones obtained by Ewins and Gleeson when a great number of points are used. Ewins and Gleeson proposed some good practices in the selection of the points in order to improve their results, but such strategy is neither robust nor programmable. This work assumes that the parameters were accurately identified in order to construct the target FRF, so that the internal product can be used instead of just selecting some isolated points.

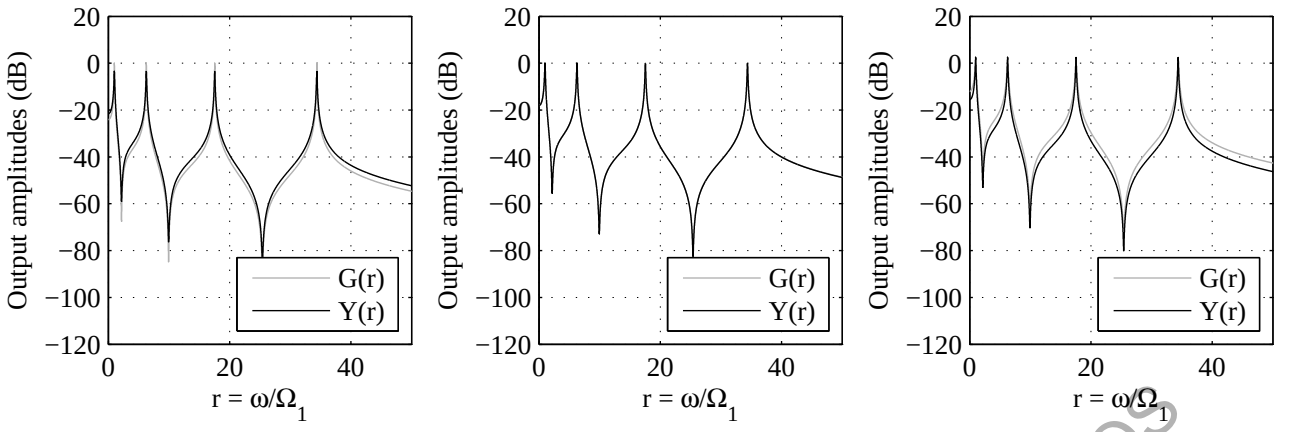

(a) Target with subestimated damping (b) Correctly identified parameters (c) Target with superestimated damping

Figure 4: Comparison of the modal sensor performance with correctly and badly identified parameters.

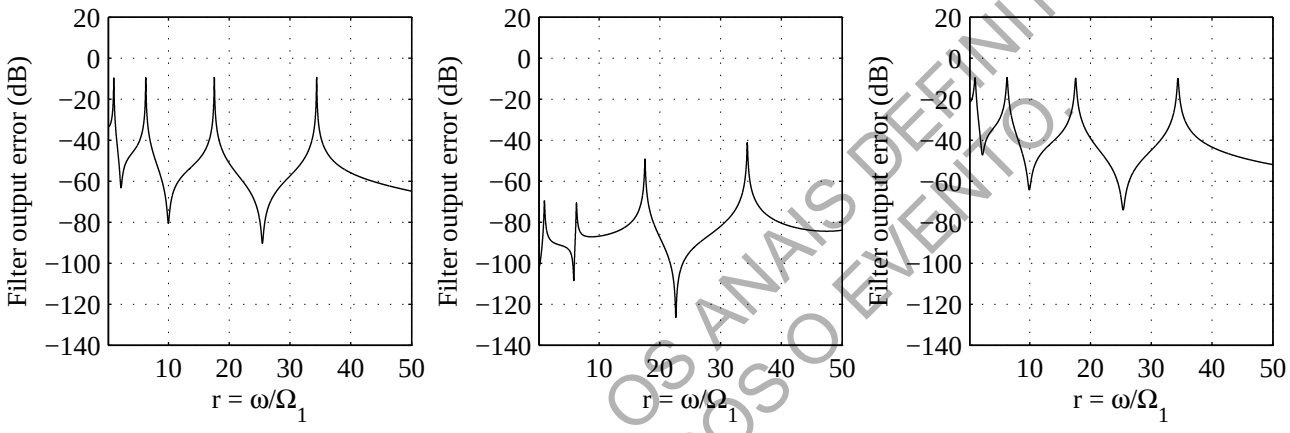

(a) Target with subestimated damping (b) Correctly identified parameters (c) Target with superestimated damping

Figure 5: Error of the modal sensor with correctly and badly identified parameters

4. OPTIMIZATION

At this point it is possible to completely define the optimization problem, as the objective function has been formulated in terms of the optmization variables.
Optimization problem:

Minimize $f_c(\mathbf{z})$ subject to:

$$\begin{array}{ll} 0 \leq \xi_1 \leq 1 & -1000 \leq \alpha_1 \leq 1000 \\ 0 \leq \xi_2 \leq 1 & -1000 \leq \alpha_2 \leq 1000 \\ \vdots & \vdots \\ 0 \leq \xi_p \leq 1 & -1000 \leq \alpha_p \leq 1000 \end{array}$$

Where:

$$\mathbf{z} = [\xi_1, \ldots, \xi_p, \alpha_1, \ldots, \alpha_p]^T$$

This non-linear optimization problem was solved by the `fmincon` function in MATLAB Optimization Toolbox. The gradient of the objective function $\nabla f_c(\mathbf{z})$ was made available to the method, since it is simple to calculate. The Hessian, however, is a bit more complicated and the method was configured to estimate it by the BFGS method.

There is one step of suboptimization being done in this method. For a predefined vector of sensor positions $\boldsymbol{\Xi}$, there is a vector of values for $\mathbf{a}$ that will minimize f_c as much as possible without moving the sensors. Those values are obtained from the Least Squares (LSQ) method, a method that was widely applied in this kind of optimization problem, as done in (Preumont *et al.*, 2003; Pagani Jr and Trindade, 2009). Complying to the previous definition of internal product, the α_j can be found by solving the following linear system:

$$\begin{bmatrix} \langle Y_1, Y_1 \rangle & \langle Y_1, Y_2 \rangle & \cdots & \langle Y_1, Y_p \rangle \\ \langle Y_2, Y_1 \rangle & \langle Y_2, Y_2 \rangle & \cdots & \langle Y_2, Y_p \rangle \\ \vdots & \vdots & \ddots & \vdots \\ \langle Y_p, Y_1 \rangle & \langle Y_p, Y_2 \rangle & \cdots & \langle Y_p, Y_p \rangle \end{bmatrix} \begin{bmatrix} \alpha_1 \\ \alpha_2 \\ \vdots \\ \alpha_p \end{bmatrix} = \begin{bmatrix} \langle G, Y_1 \rangle \\ \langle G, Y_2 \rangle \\ \vdots \\ \langle G, Y_p \rangle \end{bmatrix} \tag{17}$$

Although the optimization method will change $\boldsymbol{\Xi}$, resulting in a subsequent different $\mathbf{a}$, an initial value must be given anyways. The parameters that will suboptimize the objective function has been chosen as the best starting guess.

5. RESULTS

As a first test, the optimization was carried on with an initial vector of 4 regularly spaced points over the beam, as shown in Fig. 6a. The resulting vector of optimized parameters were then saved and the results were compared to the ones obtained from the application of the LSQ method without position optimization, that is, the modal sensor where the sensors are fixed at the initial positions and only the gains are changed.

Despite the nice improvement in the single optimization, bear in mind that this is a non-linear optimization problem, and is possibly subject to several local minima. Hoping to reduce the effect of several local minima, a second optimization was later carried on with several vectors of initial positions. They were created as all the possible combinations of 4 points out of 10 equally spaced points, resulting in a set of 210 vectors, since 10 choose 4 equals 210. Figure 6b shows one case where the points 1, 3, 7 and 10 are chosen. Then after all the cases were run, the result associated to the lowest value of the objective function was chosen from all of the local minima found. Note that this second optimization uses exactly the same method as the one used at the single optimization. The only difference resides in the way the initial conditions were organized, since there will be better chances of finding a global optimum if we try to cover the design space of the optimization variables as much as possible.

Each modal sensor design is listed in Tab. 1.

(a) Single optimization (b) Grid optimization

Figure 6: Example of initial positions

5.1 Single Optimization

This optimization showed a reasonable improvement over the design obtained from the LSQ method. The improvement can be quantitatively seen in Fig. 7b, where the reduction in the error was reasonable: from -12.83dB (22.8%) on the fifth mode, as we can see in Fig. 7a, to -20.42dB (9.53%) on the eleventh mode, as shown in Fig. 7b.

5.2 Grid optimization

Figure 7c shows that this grid optimization could reduce the maximum error to -20.68dB (9.25%), a value slightly lower than before. In the new FRF the peaks are more distributed, as if the increase in error in the other modes helped to decrease the maximum error, as we can see from the error plot appearing in Fig. 7c.

After comparing the results obtained from the single and the grid optimizations, it is clear that they are probably converging to the same configuration in the design space, since the results are really close. Then, one could wonder whether they correspond to a global minimum. Although there is not enough information to state that the new optimal configuration leads to a global minimum, given that the discretized grid contains only a finite number of points, it is possible to check the scatter plot of the obtained results and conclude that the obtained optimal is satisfactory. Figure 8a shows the final value of the objective function for each vector of initial conditions. There are basically two layers of points, one at the level where the objective function is roughly 0.02 and another around 0.002, possibly indicating the presence of two local minima. The case number which led to the lowest value of the objective function was 167, corresponding to the initial positioning at the points 3, 6, 7 and 9. In order to check if the optimization method is converging to the same optimal point, the final values of the optimization variables were also plotted as seen in Fig. 8b and 8c. Since all the points around the lower layer tend to converge to four points, for practical purposes it is a local minimum. However, at the upper layer the points a less satisfactory behavior, despite all of them concentrating around the level 0.02. Since they do not group towards fixed points, it is possible that the optimization procedure may be passing by a region of difficult convergence instead of a local minimum.

Table 1: Sensor configurations obtained from each optimization method.

Method	LSQ		Single optimization		Grid optimization	
f_c	1.13625e-2		1.81073e-3		1.79269e-3	
Sensor	Position	α_j	Position	α_j	Position	α_j
1	0.250000	-0.272484	0.188092	-0.473615	0.187048	-0.474622
2	0.500000	0.583140	0.456898	0.594436	0.456728	0.591491
3	0.750000	-0.929130	0.747410	-0.930666	0.748923	-0.939709
4	1.000000	0.489615	0.979455	0.528045	0.976760	0.538924

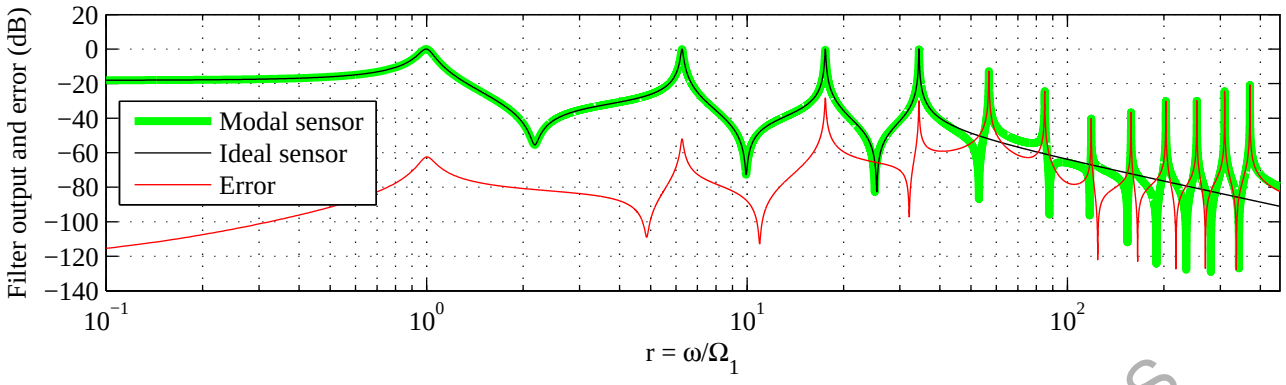

(a) Signal of modal filter with regularly space sensor whose α were calculated from the LSQ method.

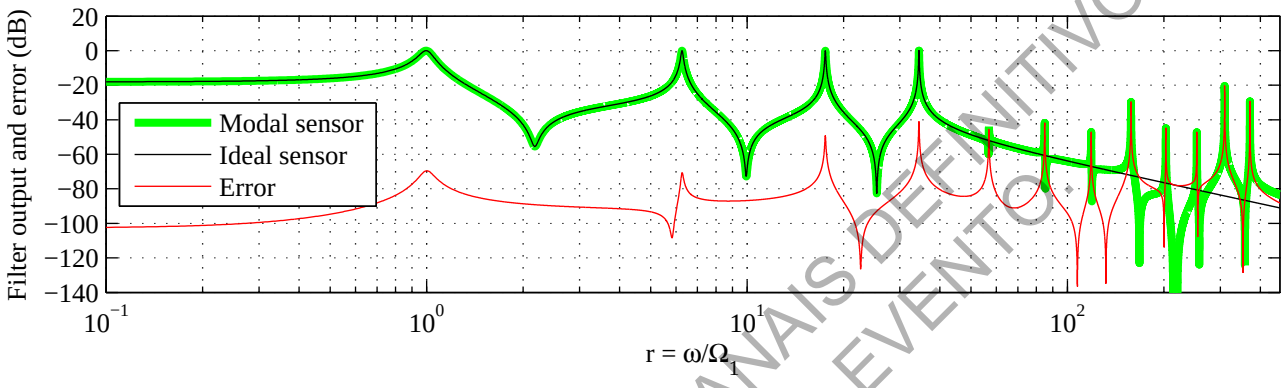

(b) Signal of the modal filter obtained from the single optimization.

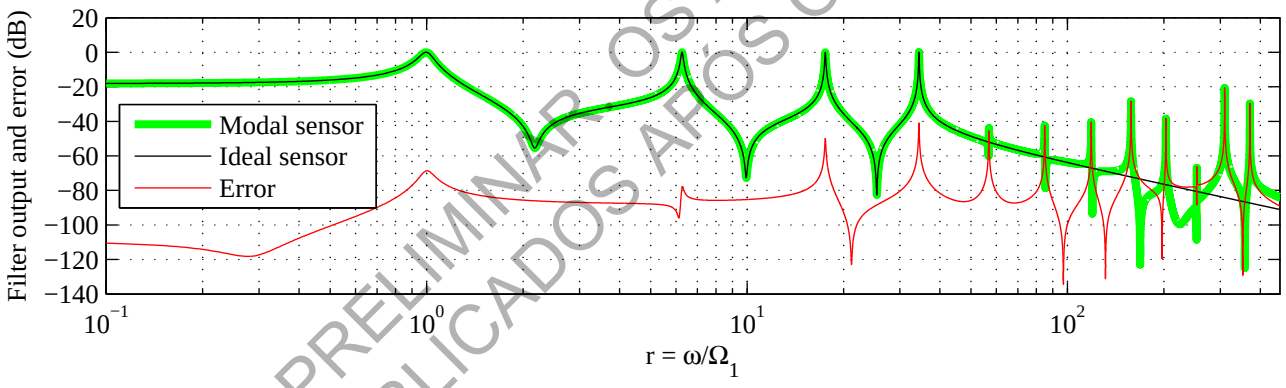

(c) Signal of the modal filter obtained from the grid optimization.

Figure 7: Comparison of the performance of the modal filters obtained from each strategy of optimization.

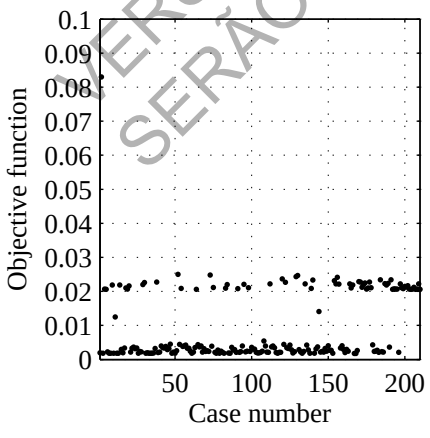

(a) The final value of the objective function versus the initial condition each identified by its case number.

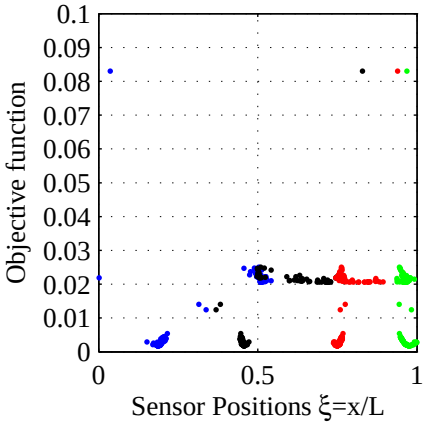

(b) The final value of the objective function versus the final sensor position

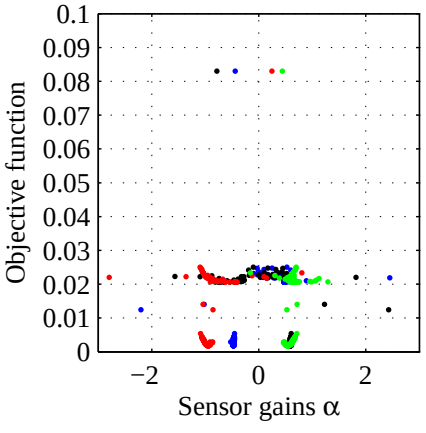

(c) The final value of the objective function versus the final value for the α.

Figure 8: Scatter plot of the results obtained from the grid optimization

6. CONCLUDING REMARKS

As shown, the optimized modal sensor was able to significantly reduce the sensor spillover caused from spatial aliasing, reducing from 22.8% in the equally spaced sensor configuration to 9.53% in the single optimization and 9.25% in the grid optimization, thus improving the performance for use in modal control.This performance may not seem outstanding, but this is a modal filter that tries to detect four modes of vibration from twelve by only using four discrete sensors. Actually, the optimal modal filter found in this study performs quite well from 0 up to $150 \cdot \Omega_1$, with no error greater than -40dB (1%) in this frequency bandwidth. Moreover, since higher modes of vibration were included in the analysis, the control engineer is able to see how badly the modal filter performs above its bandwidth in case it is chosen to be $150 \cdot \Omega_1$.

After all the optimizations, an analysis of the scatter plot showed two regions where the results tend to concentrate. One of them leads to the conclusion that the final result is probably a global minimum, while the other region could be a local minimum or just a region of difficult convergence, since the points only group vertically, but not horizontaly. During the development of the objective function it was noted that the parameters used in the definition of target FRF sharply affect the performance of the method. The detrimental impact of badly identified damping factors on the fitting of the FRF has been briefly described here.

This time the optimization was implemented on a simple beam. As for future works, the next step will consist of finding an equivalent formulation for thins plates. There is also an interest in finding a formulation that will include the effects of actuators commanded by simple control systems, such as negative velocity feedback.

7. ACKNOWLEDGEMENTS

Financial support of the MCT/CNPq/FAPEMIG National Institute of Science and Technology on Smart Structures in Engineering, grant nº574001/2008-5, is acknowledged. The first author also acknowledges CAPES for the research scholarship and Profs. M. M. Silva and P. S. Varoto for their lectures on the subject.

8. REFERENCES

Balas, M.J., 1978. "Active control of flexible systems". *Journal of Optimization Theory and Applications*, Vol. 25, No. 3, pp. 415–436.

Ewins, D.J. and Gleeson, P.T., 1982. "A method for modal identification of lightly damped structures". *Journal of Sound and Vibration*, Vol. 84, No. 1, pp. 57–79.

Friswell, M.I., 2001. "On the design of modal actuators and sensors". *Journal of Sound and Vibration*, Vol. 241, pp. 361–372.

Géradin, M. and Rixen, D., 1997. *Mechanical Vibrations: Theory and Application to Structural Dynamics*. John Wiley & Sons, Chichester, 2nd edition.

Han, J.H. and Lee, I., 1999. "Optimal placement of piezoelectric sensors and actuators for vibration control of a composite plate using genetic algorithms". *Smart Materials and Structures*, Vol. 8, No. 2, pp. 257–267.

Meirovitch, L., 1990. *Dynamics and Control of Structures*. John Wiley & Sons, Chichester.

Meirovitch, L., 1996. *Principles and Techniques of Vibrations*. Prentice Hall, New Jersey.

Meirovitch, L. and Baruh, H., 1982. "Control of Self -Adjoint Distributed-Parameter Systems". *Journal of Guidance, Control, and Dynamics*, Vol. 5, No. 1, pp. 60–66.

Pagani Jr, C.C. and Trindade, M.A., 2009. "Optimization of modal filters based on arrays of piezoelectric sensors". *Smart Materials and Structures*, Vol. 18, No. 9, pp. 1–12.

Preumont, a., François, A., De Man, P. and Piefort, V., 2003. "Spatial filters in structural control". *Journal of Sound and Vibration*, Vol. 265, No. 1, pp. 61–79.

Rao, S.S., 2009. *Engineering Optimization: Theory and Practice*. John Wiley & Sons, New Jersey, 4th edition.